The origin of the two-electron/four-centers CC bond in π-TCNE22− dimers: Electrostatic or dispersion?

ARTICLE *in* JOURNAL OF COMPUTATIONAL CHEMISTRY · JANUARY 2007

Impact Factor: 3.59 · DOI: 10.1002/jcc.20525 · Source: PubMed

3 AUTHORS, INCLUDING:

Íñigo García-Yoldi
Universidad de Navarra
13 PUBLICATIONS **207** CITATIONS

SEE PROFILE

Juan J. Novoa
University of Barcelona
276 PUBLICATIONS **5,487** CITATIONS

SEE PROFILE

The Origin of the Two-Electron/Four-Centers C—C Bond in π-$TCNE_2^{2-}$ Dimers: Electrostatic or Dispersion?

IÑIGO GARCÍA-YOLDI, FERNANDO MOTA, JUAN J. NOVOA
Departament de Química Física, Facultat de Química, and CERQT, Parc Científic, Universitat de Barcelona, Av. Diagonal 647, 08028-Barcelona, Spain

Received 10 May 2006; Revised 16 May 2006; Accepted 18 May 2006
DOI 10.1002/jcc.20525
Published online November 2006 in Wiley InterScience (www.interscience.wiley.com).

Abstract: The structure and stability of the π-$TCNE_2^{2-}$ dimers in K_2TCNE_2 aggregates is revisited trying to find if the origin of their two-electron/four-centers C—C bond are the electrostatic K^+-$TCNE^-$ interactions or the dispersion interactions between the anions. The study is done at the HF, B3LYP, CASSCF (2,2), and MCQDPT/CASSCF (2,2) levels using the 6-31+G(d) basis set. Our results show that the only minima of this aggregate that preserves the π-$TCNE_2^{2-}$ structure has the two K^+ atoms placed in equatorial positions in between the two $TCNE^-$ planes. When the K^+ atoms are placed along the D_{2h} axis of the anions the structure is not a minimum. The main energetic component responsible for the stability of these aggregates comes from the cation–anion interactions. However, a proper accounting of the dispersion component (as done in the MCQDPT/CASSCF (2,2) calculations) is needed to make the closed-shell singlet more stable than the open-shell singlet. Thus, the bond results from the combination of the electrostatic and dispersion components, being the first the dominant one. The optimum geometry of the closed-shell singlet is very similar to the experimental one found in crystals.

Key words: π-$TCNE_2^{2-}$dimers; two-electron/four-centers C—C bond; long C—C bonds; interaction energy; HF; B3LYP; CASSCF; MCQDPT calculations

Introduction

Since it was first reported[1] in some ionic crystals, the existence of two-electron/four-centers (2e/4c) long distance C—C bond between pairs of $TCNE^-$ anion-radicals has been firmly established, based of various theoretical and experimental studies.[2–9] One example of crystal where this type of bond is found is the $K_2TCNE_2glyme_2$ crystal,[10] where one finds K_2TCNE_2 aggregates that clearly show the presence of π-$TCNE_2^{2-}$ dimers (Fig. 1). The existence of 2e/4c C—C bonds in these dimers explains many of the experimental properties observed in ionic crystals that present these dimers, the most relevant one being the diamagnetic nature of the π-$TCNE_2^{2-}$ dimers. However, as we discuss later, the origin of the 2e/4c C—C bond in π-$TCNE_2^{2-}$ dimers is still a matter of debate. Our aim in this work is to shed light into such discussion.

Initially,[1] the existence of 2e/4c C—C bonds was associated to the cation–anion interactions between the two $TCNE^-$ monomers that form the π-$TCNE_2^{2-}$ dimers and their surrounding cations (Fig. 2). As results of these cation–anion interactions, the two anions move to short distances, where their π^* SOMO orbitals, are forced to a direct overlap. Such forced overlap gives rise to the molecular orbital diagram shown in Figure 2. All these effects are already present is small $cation_2anion_2$ aggregates. Consequently, the K_2TCNE_2 aggregate of Figure 1 can serve to understand the properties and energetics of the aggregates found in the K_2TCNE_2-$glyme_2$ crystal.

The four fragments that constitute the K_2TCNE_2 aggregate are charged. Therefore, one expects that the three types of fragment–fragment interactions that they can make (cation–anion, anion–anion, cation–cation) should be dominated by the electrostatic component. On the basis of this idea, we initially performed[1] UHF,[11] UB3LYP, (B3LYP is a density functional obtained by taking the three parameter non-local exchange funcional of Becke and the non-local correlation functional of Lee-Yang-Parr)[12] and CASSCF(6,4) calculations[11] using the 6-31+G and 6-31+G(d) basis sets (these methods provide a proper description of the electrostatic component). They showed that (1) the interaction between two isolated $TCNE^-$ radical-anions is repulsive at all monomer–monomer distances (a metaestable minimum is found at the RHF but disappears when the double occupancy condition is relaxed), (2) at the geometry of the π-$TCNE_2^{2-}$ dimers found in the crystals,

Correspondence to: J. J. Novoa; e-mail: juan.novoa@ub.edu

Contract/grant sponsor: Spanish Science and Education Ministry; contract/grant numbers: BQU2002-04587-C02-02, CTQ2005-02329

Contract/grant sponsor: Catalan Autonomous Government; contract/grant numbers: 1999SGR-00046, 2005SGR-00036

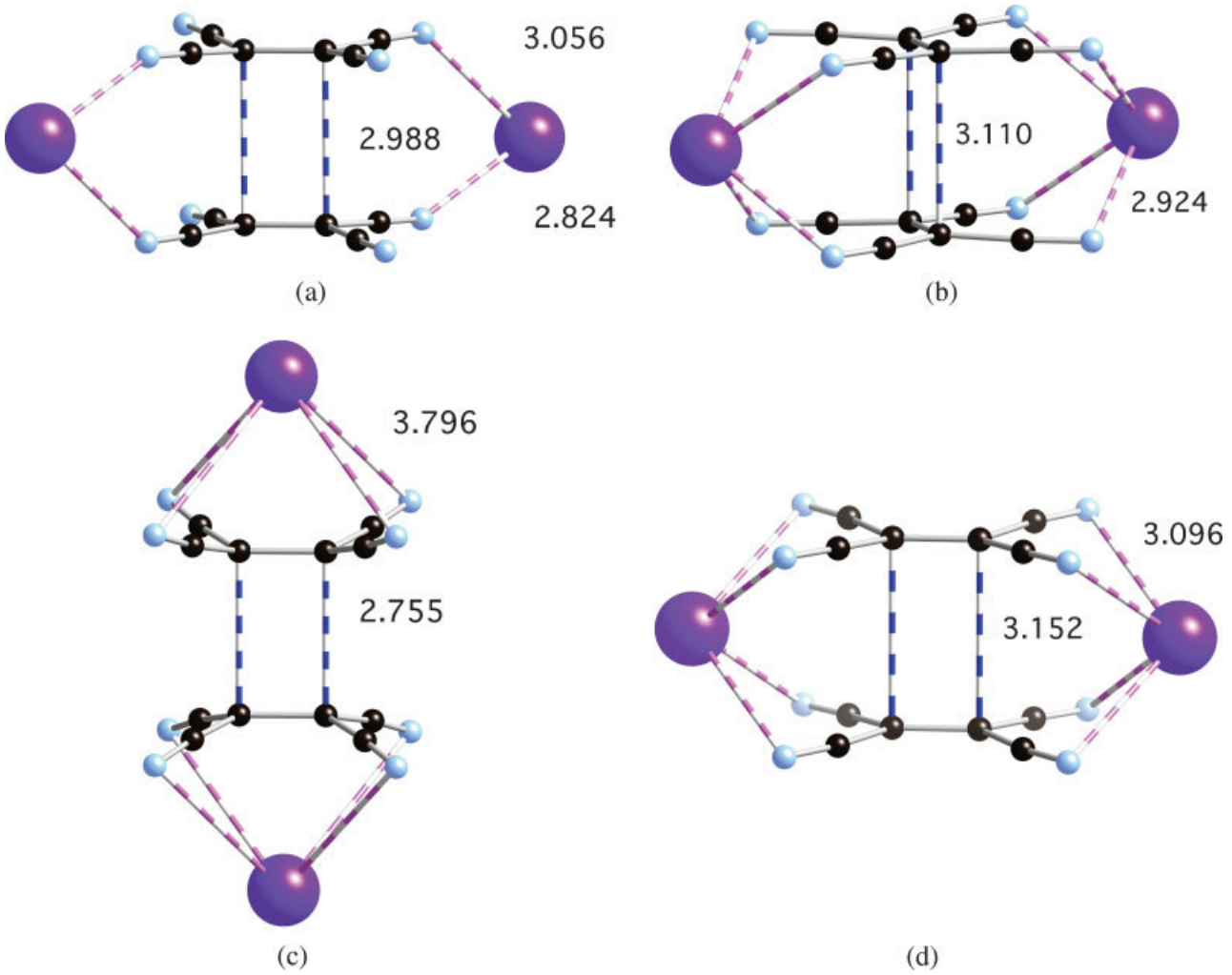

Figure 1. Geometry of the $(K^+)_2TCNE_2^{2-}$ aggregates used in this work: (a) Geometry found in the KIYHIJ crystal (notice the equatorial position of the two K^+ atoms, and the outward orientation of the CN groups). (b) Optimum geometry of the more stable equatorial aggregate computed at the RB3LYP/6-31+G(d) level. (c) Optimum geometry of the axial aggregate optimized at the RB3LYP/6-31+G(d) level. (d) Optimum geometry of the less stable equatorial aggregate computed at the RB3LYP/6-31+G(d) level. The shortest C···C distance between the anions and the K^+···N distance have been indicated (in Å).

the B3LYP interaction energy is 34.6 kcal/mol more stable than the UHF interaction, (3) the overall interaction energy of the K_2TCNE_2 aggregate is −158.4 kcal/mol (UHF/6-31+G(2d, 2p) calculation, negative values indicate stable aggregates; values of the same order are found with other methods and basis sets), and (4) the bonding properties of the cation-induced 2e/4c C—C bond in π-$TCNE_2^{2-}$ dimers originate on the similar molecular orbital diagram for the $TCNE^-$···$TCNE^-$ interactions and that found in energetically stable dimers. For the usual ion–ion interactions the MP2 interactions energies (which are known to include more than 90% of the dispersion component) are taken as reference values. In these cases the Hartree-Fock and B3LYP values are very close to the MP2 results. However, the radical nature of the $TCNE^-$ anions questions if the situation is still valid in the $TCNE^-$···$TCNE^-$ interactions.

Full geometry optimizations at the UHF or UB3LYP levels give aggregates similar to the experimental ones (compare Figs. 1a and 1b), with the K^+ atoms placed equatorially in between the two $TCNE^-$ anions and the CN groups pointing outwards, as is found in the crystal. Similar results are found independently of the cation (K^+, Et_4N^+, and Tl^+).[1] The stability of the optimum structure of these aggregates against a dissociation into their four constituent monomers is also similar (between −120 and −160 kcal/mol) when the cation is changed, close to that found when using the crystal geometry. Notice that these values should not be compared with the values of the enthalpy of dimerization in solution (7.9 kcal/mol in dichloromethane at 298 K[7]) as the two originate in different interactions (in solution the energy that counterbalances the $TCNE^-$···$TCNE^-$ repulsion is the attractive anion–solvent interaction).[13] Initial B3LYP calculations on $TCNE_2^{2-}$ (dichloromethane)$_6$

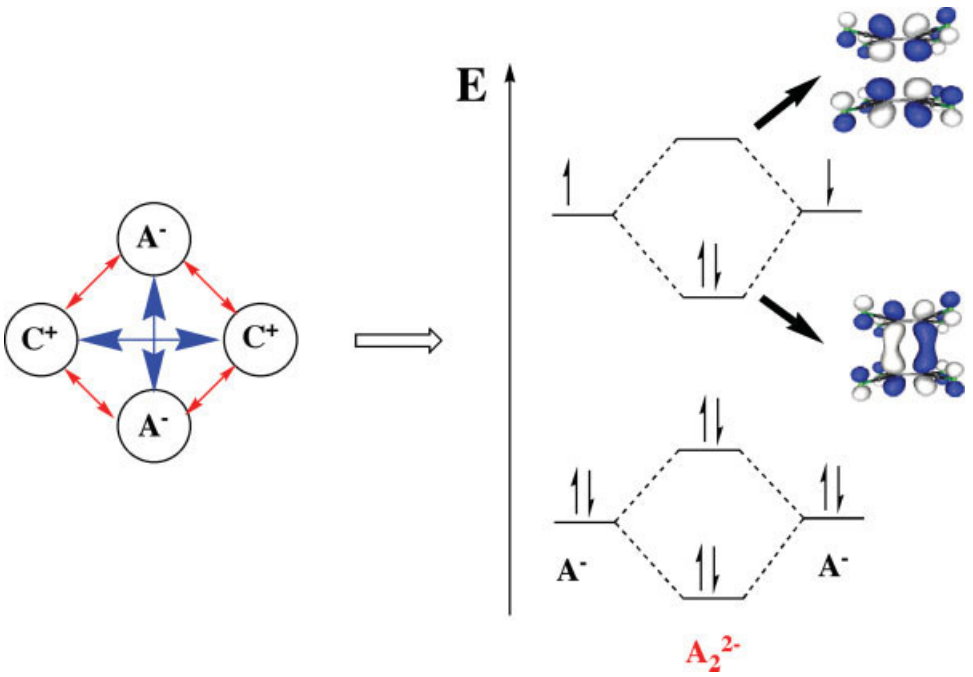

Figure 2. Molecular orbital diagram for the $TCNE^{-}\cdots TCNE^{-}$ interaction for the region of the SOMO orbital of the $TCNE^{-}$ fragments (the diagram in this region is identical for two isolated $TCNE^{-}$ monomers and for two monomers combined with two K^{+} atoms).

aggregates in their triplet state found slightly stable aggregates, −1.1 kcal/mol, but more stable aggregates are expected to be found when dispersion is properly accounted for; see ref. 13.

The electrostatic nature of the cation-induced 2e/4c C—C bonding properties in $TCNE^{-}\cdots TCNE^{-}$ interactions was later on questioned,[9] claiming that "the long C—C bond observed in π-$TCNE_2^{2-}$ dimers is in fact an outcome of significant dispersion attractions between the two cofacial monomers." The authors reached this conclusion by analyzing the interaction energy of a K_2TCNE_2 aggregate having its two K^{+} atoms in axial positions (in the following, the axial K_2TCNE_2 aggregate, Fig. 1c). More specifically, they compared the perfect paring (PP) interaction energy curve with that obtained by doing a second-order Moller-Plesset calculation on the perfect-pairing wavefunction[14] for the dissociation of K_2TCNE_2 into two ($K^{+}TCNE^{-}$) units. The later method is a specific case multireference quasidegenerate perturbative theory implementation (MCQDPT) that when applied to a PP wavefunction gives results similar to a CASPT2 calculation[15] done on a CASSCF(2,2) wavefunction. We should mention here that the MCQDPT/PP method makes a proper evaluation of the dispersion component, while the PP does not include such component. It was found that while the PP interaction curve is always repulsive, the MCQDPT/PP curve has an attractive minimum when the C···C distance is 2.6 Å with interaction energy of −17.3 kcal/mol (6-31G(d) values, similar values are found with other basis). It does not disappear when the BSSE is corrected (the minimum drifts to 2.7 Å and the BSSE-corrected interaction energy becomes −11.2 kcal/mol). The authors pointed the similarity between these values and the enthalpy for the formation of $TCNE^{-}$ dimers found in solutions of dichloromethane (−8.8 kcal/mol[7]) a fact that they took as a confirmation of their theoretical results. On isolated π-$TCNE_2^{2-}$ dimers, the PP calculations found no minimum while the MCQDPT/PP calculations found a weak metaestable dimer only marginally stable. Therefore, dispersion plays a role, but it is not enough to justify the existence of isolated π-$TCNE_2^{2-}$ dimers, while once two K^{+} cations are added the aggregate becomes energetically stable. This suggests that cation–anion interactions are more important in stabilizing the π-$TCNE_2^{2-}$ dimers than dispersion. On top of this, another weak point of this study is the fact that it is done on the axial $(K^{+})_2TCNE_2^{2-}$ aggregates, because no axial aggregates are found in any of the crystal structures deposited in the Cambridge Crystallographic Database[16] (all crystals present equatorial aggregates).

Given such a situation, we decided to reinvestigate the origin of the existence of π-$TCNE_2^{2-}$ dimers using also MCQDPT methods but on the equatorial π-$TCNE_2^{2-}$ conformation. We first started our work by investigating in a systematic form the shape of the potential energy surface of the K_2TCNE_2 aggregates, trying to test if the axial and the equatorial conformations are local minima on this surface. Then, we computed the interaction energy curve for the dissociation of the equatorial aggregates (the only minimum) into two ($K^{+}TCNE^{-}$) units using various methods: (HF, B3LYP, CASSCF and MCQDPT), trying to evaluate the relative importance of the cation–anion interactions and the dispersion component in defining the stability of the π-$TCNE_2^{2-}$ dimers. This evaluation can be done by comparing at the curves computed with methods that make a proper accounting of dispersion (like the MCQDPT method, which also makes a proper evaluation of the electrostatic component) with the HF and CASSCF curves (that do not include dispersion, but properly account for

the electrostatic component), or with the B3LYP curve (that includes only part of the total dispersion and also makes a proper accounting of the electrostatic component). This analysis is necessarily qualitative and based upon the assumption that these methods provide a similar description of the electrostatic component.

Methodology

We will only focus on π-TCNE$_2^{2-}$ dimers and K_2TCNE_2 aggregates in their singlet state, given the fact that experimentally it is well know that when π-TCNE$_2^{2-}$ dimers are formed they become diamagnetic (that is, the spin state of the dimer is $S = 0$).

The aggregates under investigation are composed of ionic fragments. The Hartree-Fock[11] and B3LYP[12] density functional[17] are known to provide a good description of the interaction energy in systems where the most important energetic component is the electrostatic one. Therefore, we used these methods in our initial studies. As previous studies[8,9] have indicated that a proper inclusion of the dispersion component can be relevant in studying the π-TCNE$_2^{2-}$ dimers, we will also carry out MCQDPT calculations[14] on a CASSCF(2,2) wavefunction[14] (MCQDPT/CASSCF(2,2) calculations). Notice that MCQDPT/CASSCF(2,2) calculations give results similar to MCQDPT/PP calculations and provide an accurate accounting of the dispersion component of the interaction energy. Besides, the CASSCF(2,2) wavefunction provides a proper description of the open-shell (diradical) singlet at all distances.

We have done the HF and B3LYP calculations in two forms: by imposing the double occupancy condition of the orbitals (RHF and RB3LYP calculations), and then by releasing such condition (UHF and UB3LYP calculations). In the later two calculations, we have always checked if a broken-symmetry solution exists,[18,19] to allow the system falling into the open-shell singlet state when it is more stable. It is known that the B3LYP potential energy surface computed using the broken-symmetry approximation mimics that obtained in CASSCF calculations.[20]

All calculations were done using the 6-31+G(d) basis set. A basis set built by adding diffuse functions to the 6-31G(d) basis set.[21] The HF and B3LYP calculations were done using the and the appropriate options in Gaussian-03,[22] while the CASSCF and MCQDPT/PP calculations were done using the appropriate options in GAMESS[23] (we found that this multireference perturbative implementation produces a smoother potential energy surface than other MCQDPT implementations available to us). When required, the basis set superposition error (BSSE) will be corrected using the counterpoise method.[24–26]

Results and Discussion

Optimum Structure of the K_2TCNE_2 Aggregates that Preserve the π-TCNE$_2^{2-}$ Dimers

We first fully optimized the geometry of the equatorial and axial conformations of the K_2TCNE_2 aggregate at the RHF and RB3LYP levels. No symmetry was imposed in the optimization of the equatorial conformer, while a D_{2h} symmetry was used in the axial conformer. The B3LYP optimum geometries are shown in Figures 1b–1d. Two nonequivalent conformers are possible in the equatorial conformation, which only differ in the relative position of the K^+ cations (Figs. 1b and 1c). The most stable one (by 31.3 kcal/mol at the B3LYP level) has its two K^+ cations placed laterally relative to the central C—C bond of each $TCNE^-$ fragment. From now on we will only focus in the most stable conformer, as both equatorial conformers are expected to present similar properties in relation to the origin of their stability.

At the RB3LYP level, the formation energy of the optimum geometry of the axial form is −146.6 kcal/mol, that is, the aggregate is stable against its dissociation into its four fragments. In this work we will use the term formation energy to indicate the difference between the energies of the aggregate and its fragments all at their optimum geometry. The interaction energy will be used to indicate the same energy difference but when the fragments are aggregate are taken at the optimum geometry of the aggregate. However, it is slightly unstable (0.3 kcal/mol) for its dissociation into two ($K^{+\cdots}TCNE^-$) units. On the other hand, at the RB3LYP level the most stable equatorial conformation is 60.3 kcal/mol more stable than the axial conformation. This higher stability of the equatorial form is consistent with electrostatic considerations about the most stable way of placing two (K^+TCNE^-) units. A vibrational analysis of the optimum geometries of the equatorial and axial conformers shows that only the equatorial conformer is a true minimum, while the optimum geometry of the axial conformer presents three negative eigenvalues at the B3LYP level. This, together with the lower stability of the axial conformation relative to the equatorial one, explains why no axial conformers are found in the crystals.

To search for other possible minimum energy conformers that preserve the structure of π-TCNE$_2^{2-}$ dimers, we now explored (at the UHF and UB3LYP levels) the region of the potential energy surface of the K_2TCNE_2 aggregate that connects the equatorial and axial conformers. As we were only interested in structures preserving the π-TCNE$_2^{2-}$ dimers, the search was done by synchronously rotating the position of the two K^+ cations respect to the mirror plane placed in-between the planes of the two $TCNE^-$ fragments (coordinate θ in Fig. 3). During this scan the π-TCNE$_2^{2-}$ geometry was frozen at the optimum for the equatorial conformation. The scan was done for various distances between the K^+ cations and the center-of-mass of the π-TCNE$_2^{2-}$ dimer (coordinate r in Fig. 3). The shape of the UHF and UB3LYP (r, θ) potential energy surface (Fig. 4) indicates that the equatorial conformation is the only minimum in this surface. The axial conformation is a saddle point, in good agreement with the results of the vibrational analysis described before.

It is also worth pointing here that we have found two other local minimum energy structures on the K_2TCNE_2 potential energy surface, but none of them preserves the π-TCNE$_2^{2-}$ dimer structure: (a) the σ-TCNE$_2^{2-}$ dimer structure, in which a classical C—C covalent bond is formed (r_{C-C} = 1.616 Å) between the two radical-anions,[1] and (b) a $K^{+\cdots}TCNE^{-\cdots}$ $K^{+\cdots}TCNE^-$ intercalated structure. We will not pay more attention to them, as they are out of the scope of this paper.

The Origin of the Stability in the Equatorial Conformation of the K_2TCNE_2 Aggregates

Once we have shown that the equatorial conformation is the only minimum energy structure on the K_2TCNE_2 surface that pre-

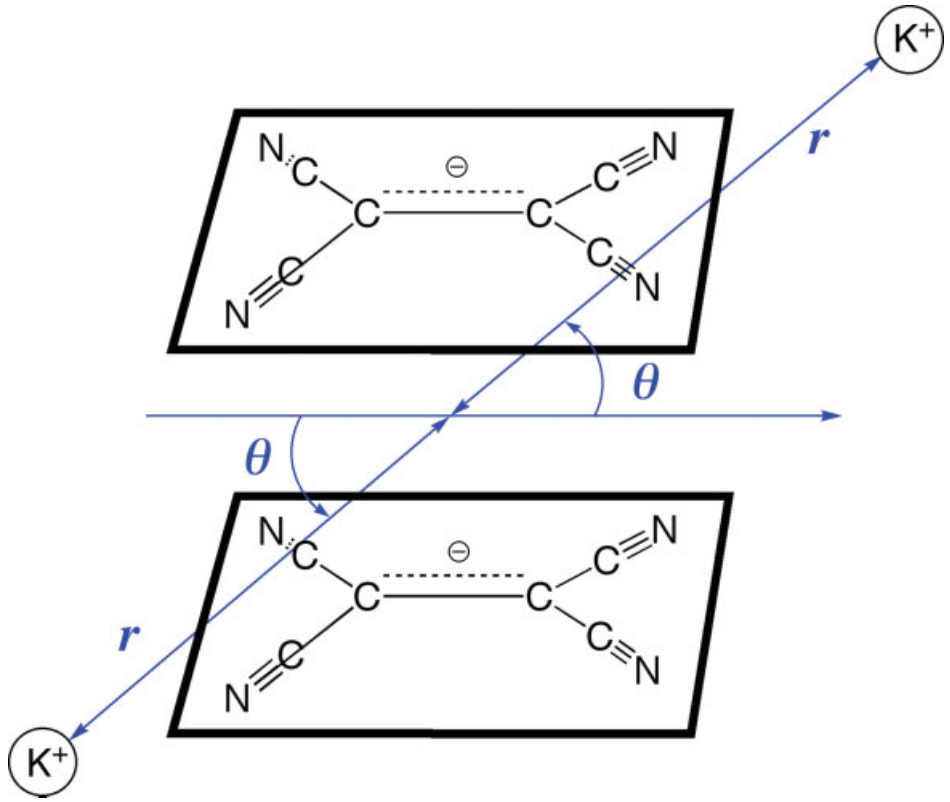

Figure 3. Coordinates employed in the scan of the potential energy surface that connects the equatorial and axial conformations. [Color figure can be viewed in the online issue, which is available at www.interscience.wiley.com.]

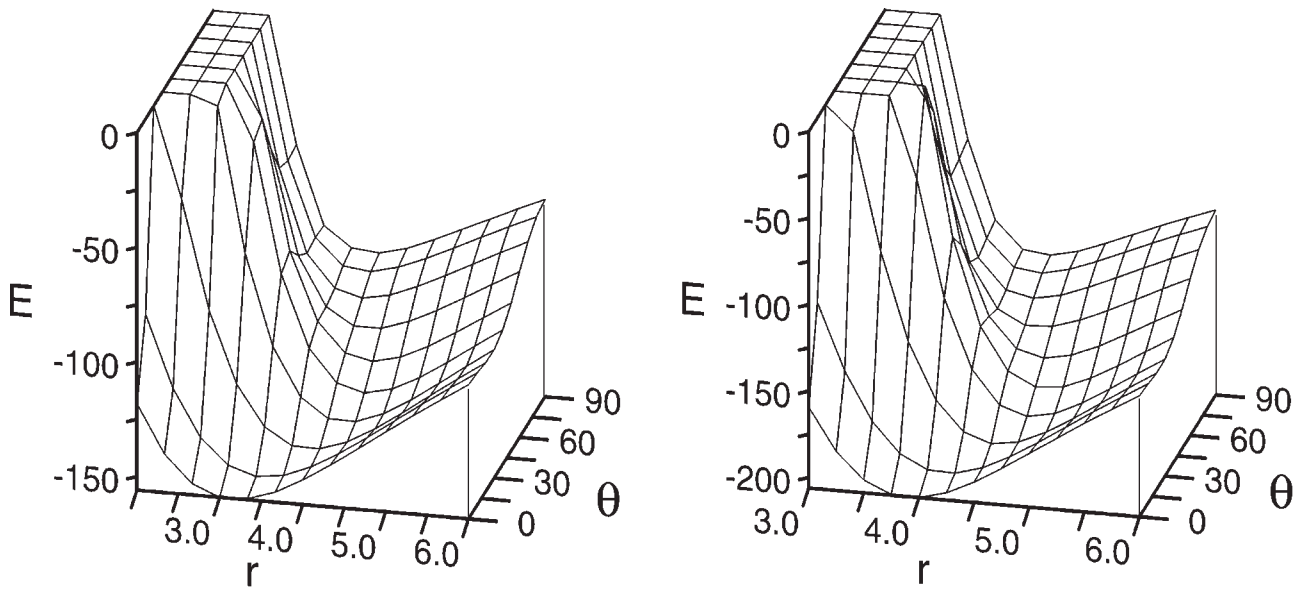

Figure 4. Shape of the $E(r,\theta)$ potential energy surface that connects the equatorial ($\theta = 0°$) and axial ($\theta = 90°$) conformations. Left: HF surface. Right: B3LYP surface (the optimum value of r for both conformations changes with the method). The energy plotted are formation energies (that is difference between the energy of the K_2TCNE_2 aggregate at the geometry of interest and the sum of the optimum energy of two K^+ and two $TCNE^-$ fragments at their optimum geometries).

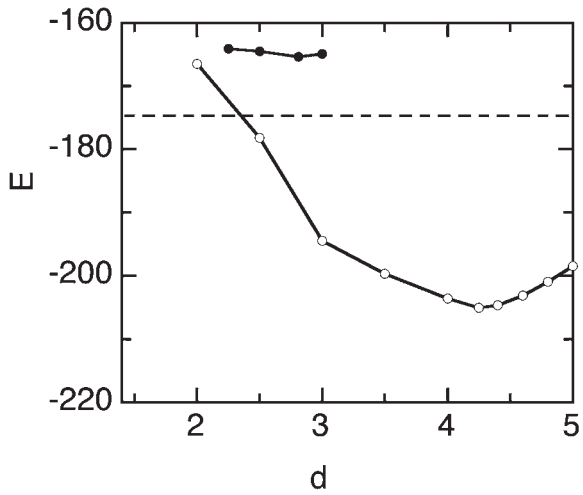

Figure 5. Potential energy curve for the dissociation of a K_2TCNE_2 aggregate into two ($K^{+\cdots}TCNE^-$) units. Open circles: opens-shell singlet (UHF calculations); filled circles: closed-shell singlet (RHF calculations). The values of *E* (kcal/mol) correspond to the formation energy of the K_2TCNE_2 aggregate respect to its four constituent fragments at their optimum geometry. The values of *d* (Å) refer to the C$^{\cdots}$C distance between the central carbon atoms of each $TCNE^-$ fragment. The broken line marks the formation energy of two isolated ($K^{+\cdots}TCNE^-$) units (−175.5 kcal/mol).

serves the structure of π-TCNE$_2^{2-}$ dimer, we will now study the origin of its stability, trying to find the relative importance of the dispersion interactions (which originate on the anion–anion interaction, that is, within the π-TCNE$_2^{2-}$ dimer) and the cation–anion interactions (that is, the K^+-$TCNE^-$ interactions). We will do this study only for the most stable equatorial conformation.

One way of evaluating the importance of the dispersion term is by subtracting the potential energy curves for the dissociation of the K_2TCNE_2 aggregate into two (K^+TCNE^-) units computed at the HF and MCQDPT/CASSCF(2,2) levels. Furthermore, for comparative purposes, we also did B3LYP calculations. We performed the HF and B3LYP calculations at the RHF and RB3LYP calculations (which describe only closed shell singlet states) and at the UHF and UB3LYP curves (where one can describe open-shell singlet states). We will not do calculations on the isolated π-TCNE$_2^{2-}$ dimer, because its properties are already known from previous studies (the dimer is repulsive at all distances when computed at the HF, B3LYP, CASSCF,[1] PP, and MCQDPT/PP[9] levels, but the MCQDPT/PP curve presents a shallow metaestable minimum that practically disappears when the BSSE is corrected).

Figures 5–7 present the shape of the potential energy curves for the dissociation of a K_2TCNE_2 aggregate into two ($K^{+\cdots}TCNE^-$) units computed at the HF, B3LYP, CASSCF(2,2), and MCQDPT/CASSCF(2,2) calculations. We started by doing exploratory calculations at the HF level (Fig. 5), complemented by calculations at the B3LYP level (Fig. 6). Two sets of curves were computed: (1) the RHF and RB3LYP curves for the closed-shell singlet, and (2) the UHF or UB3LYP curves for the open-shell singlet (obtained from the RHF solution by mixing the HOMO and LUMO orbitals of the RHF calculation). There are two main features in these curves:

a. The UHF, RB3LYP, and UB3LYP curves are more stable than two isolated ($K^{+\cdots}TCNE^-$) units. Therefore, given the fact that the HF method does not include dispersion, we can conclude that dispersion is not needed to justify the stability of the K2TCNE2 equatorial conformer. This leaves the cation–anion interactions as the main driving force behind the origin of these aggregates (and the 2e/4C C—C bond present in the π-TCNE$_2^{2-}$ dimers that they contain).
b. The HF and B3LYP calculations predict that the closed-shell singlet state (optimum structure shown in Figs. 1b–1d) is less stable than the open-shell singlet state. A Mulliken population analysis confirmed that in the open-shell state both $TCNE^-$ fragments had a −1 au net charge and total atomic spin population of +1 and −1 au, as corresponds to an open-shell singlet.

The optimum UB3LYP geometry of the open-shell singlet (Fig. 8, the optimum HF geometry is similar) presents two remarkable differences respect to the π-TCNE$_2^{2-}$ dimers detected in crystals (Fig. 1a): (a) the C$^{\cdots}$C distance between the central atoms of the $TCNE^-$ fragments (4.033 Å) is about 1 Å larger, and (b) the $TCNE^-$ fragments are bent inwards, contrary to the outwards bending that the π-TCNE$_2^{2-}$ dimers present in crystals. To fully characterize the bonds in the open-shell and closed-shell minima, we carried out an atoms-in-molecules analysis of the electronic densities of these structures at their optimum geometry. In both minima the two K^+ atom present four K$^{\cdots}$N (3,−1) bond critical

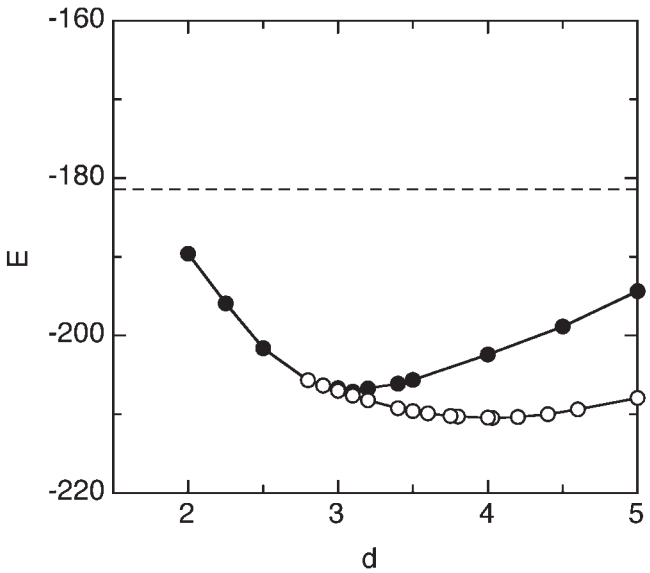

Figure 6. Potential energy curve, computed using the B3LYP functional, for the dissociation of a K_2TCNE_2 aggregate into two ($K^{+\cdots}TCNE^-$) units. Open circles: opens-shell singlet (UHF calculations); filled circles: closed-shell singlet (RHF calculations). The values of *E* (kcal/mol) correspond to the formation energy of the K_2TCNE_2 aggregate respect to its four constituent fragments at their optimum geometry. The values of *d* (Å) refer to the C$^{\cdots}$C distance between the central carbon atoms of each $TCNE^-$ fragment. The broken line marks the formation energy of two isolated ($K^{+\cdots}TCNE^-$) units (−181.5 kcal/mol).

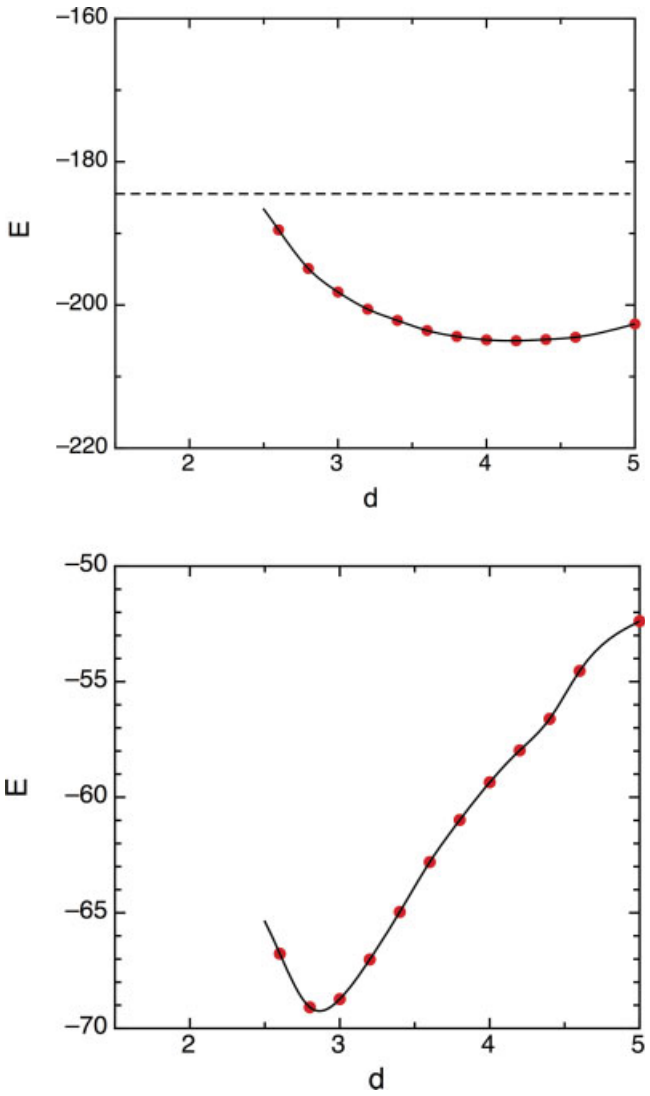

Figure 7. Up: Potential energy curve, computed at the CASSCF(2,2) for the dissociation of a K_2TCNE_2 aggregate into two ($K^{+\cdots}TCNE^{-}$) units. The values of *E* (kcal/mol) correspond to the formation energy of the K_2TCNE_2 aggregate respect to its four constituent fragments at their optimum geometry. The broken line marks the formation energy of two isolated ($K^{+\cdots}TCNE^{-}$) units (−186.9 kcal/mol). Down: Potential energy curve, computed at the MCQDPT/CASSCF(2,2) for the dissociation of a K_2TCNE_2 aggregate into two ($K^{+\cdots}TCNE^{-}$) units. The values of *E* (kcal/mol) directly correspond to the formation energy of the K_2TCNE_2 aggregate respect to *i* two ($K^{+\cdots}TCNE^{-}$) units at their optimum geometry. The values of *d* (Å) in both cases refer to the $C^{\cdots}C$ distance between the central carbon atoms of each $TCNE^{-}$ fragment. In this energy scale, the formation energy of two isolated ($K^{+\cdots}TCNE^{-}$) units is equal to zero. [Color figure can be viewed in the online issue, which is available at www.interscience.wiley.com.]

points. Given the attractive nature of the $K^{+\cdots}TCNE^{-}$ interactions, we can conclude that each bond critical point is associated to an intermolecular $K^{\cdots}N$ ionic bond. In the closed-shell singlet state one also finds two $C^{\cdots}C$ (3,−1) bond critical point connecting the central atoms of the $TCNE^{-}$ fragments (placed within the funnels shown in Fig. 9). In previous studies these critical points were associated to the 2e/4c C—C bonds.[1] The density on these critical points is 0.012 au These $C^{\cdots}C$ funnels and their (3,−1) bond critical points are also found in the open-shell singlet structure, although with a much smaller density at the critical point (0.002 au). However, in the later case these $C^{\cdots}C$ (3,−1) bond critical points cannot be associated to a bond because attractive interaction can exist between two electrons in an open-shell singlet configuration and the electrostatic interaction is clearly repulsive. Thus, the optimum structure of the open-shell singlet differs from the optimum closed-shell structure in the absence of the central 2e/4c C—C bond.

Once the electronic structure of the closed-shell and open-shell optimum structures are understood, we can rationalize the features found in the potential energy curves shown in Figures 5 and 6. In the HF calculation, the closed shell stability is not properly described (this method does not include dispersion and it is known that dispersion is relevant for the stability of the 2e/4c C—C bonds[8,9]). Thus, the stability of the closed-shell structure is grossly underestimated at the HF level. Such a fact is partially corrected in the B3LYP calculations, where the closed-shell singlet becomes just 3 kcal/mol less stable than the open-shell singlet. In the open-shell singlet the only intermolecular bonds are the cation–anion bonds, while the closed-shell structure also has a 2e/4c C—C bonds connecting the two anions. The closed-shell structure presents a shorter $C^{\cdots}C$ distance, but the extra C—C bond is not associated to a higher stability (the inwards bending of the $TCNE^{-}$ fragments in the open-shell singlet allows a longer distance between atoms that host a net negative charges, thus minimizing their repulsive interaction). All facts suggest a failure of the HF and B3LYP calculations to properly account for the stability of such structure (probably due to a failure to properly account for the dispersion component of the interaction energy). Therefore, to test this possibility we decided to perform MCQDPT/CASSCF(2,2) calculations, whose main difference with the CASSCF(2,2) computations is placed in a proper inclusion of the dispersion component of the interaction energy.

The computed MCQDPT/CASSCF(2,2) potential energy curves are plotted in Figure 7. The curves were computed at the optimum

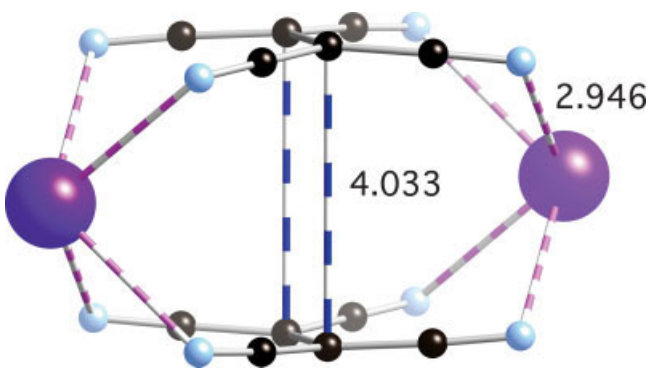

Figure 8. Optimum geometry for the open-shell singlet of the equatorial aggregate computed at the UB3LYP/6-31+G(d) level. The shortest $C^{\cdots}C$ distance between the anions and the $K^{+\cdots}N$ distance have been indicated (in Å).

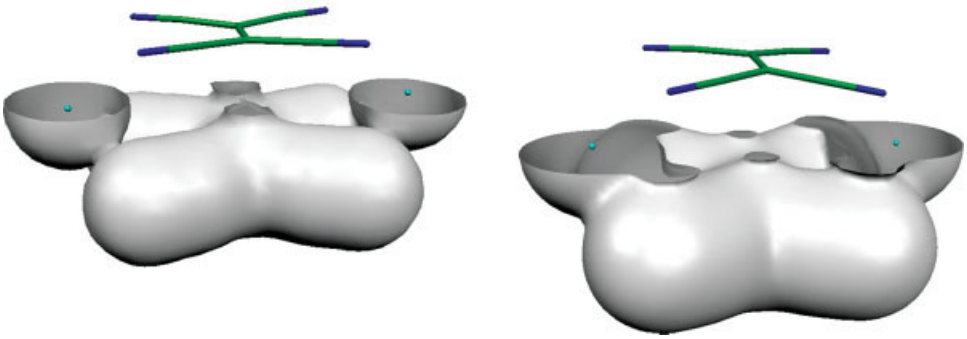

Figure 9. Electron density distribution for the closed-shell singlet (left) and open-shell singlet (right) states of the K_2TCNE_2 aggregate at their UB3LYP optimum geometries. In the closed, the surface of 0.02 au is plotted in the closed-shell case, while in the open-shell case it is the surface of 0.0025 au. For a more clear understanding of the pictures, only the density around the lowest half of the aggregate is plotted. Notice the funnels connecting the two $TCNE^-$ fragments.

UB3LYP optimized geometry for each point, as a MCQDPT/CASSCF(2,2) optimization of the K_2TCNE_2 structure is currently prohibitive for us. We first analyze the CASSCF(2,2) curve (upper part of Fig. 7). It presents a clear similarity with the UB3LYP curve, and has only one minimum at 4.2 Å, whose electronic structure is that for an open-shell singlet (the occupation of the two natural orbitals is 1.14 and 0.86, also indicating a non-negligible multireference behavior). The MCQDPT/CASSCF(2,2) curve is strikingly different than the HF, B3LYP, or CASSCF(2,2) curves: (a) the closed-shell singlet structure becomes more stable than the open-shell singlet, being the only minimum in the potential energy curve (at 2.8 Å, at this geometry the occupation of the two natural orbitals is 1.75 and 0.25, also showing a non-negligible multireference character of the wavefunction), and (b) the CASSCF(2,2) and MCQDPT/CASSCF(2,2) curves are placed below the limit of dissociation of the K_2TCNE_2 aggregate into two isolated ($K^{+\cdots}TCNE^-$) fragments (notice that the MCQDPT/CASSCF(2,2) has been computed as energy increment from two isolated ($K^{+\cdots}TCNE^-$) units due to the errors that this method presents when computing an isolated $TCNE^-$ anion). At $r = 2.8$ Å UB3LYP and RB3LYP curves are the same and, in consequence, the geometry of the K_2TCNE_2 system at 2.8 Å is that for the closed-shell singlet minimum, shown in Figure 1b. Therefore, a proper accounting of the dispersion component (as that done at the MCQDPT/CASSCF(2,2) level) is required to obtain a closed-shell singlet minimum energy structures for the π-TCNE$_2^{2-}$ dimer, in good agreement with the experimental structures found in crystals. The size of the dispersion component can be estimated from the difference between the CASSCF(2,2) and MCQDPT/CASSCF(2,2) curves, placed in the same energy scale. We have estimated that for the closed-shell structure is 61.1 kcal/mol, which can be compared with a total formation energy of −256.0 kcal/mol, respect to the four fragments (or just −8.9 kcal/mol respect to two isolated ($K^{+\cdots}TCNE^-$) units). Therefore, the stability of the aggregate is already achieved by the electrostatic interactions present in the CASSCF(2,2) calculations. This is, consequently, the main driving force behind the stability of the π-TCNE$_2^{2-}$ dimers in equatorial K_2TCNE_2 conformations, that is, behind the existence of 2e/4C C—C bonds in these aggregates. However, a proper description of the origin of this bond also requires of an accurate evaluation of the dispersion component.

Concluding Remarks

The results of HF, B3LYP, CASSCF(2,2), and MCQDPT/CASSCF(2,2) calculations on K_2TCNE_2 aggregates indicate the following main facts: (1) the axial conformation is not a minimum energy structure, (2) there are two minimum energy structures of these aggregates in which the π-TCNE$_2^{2-}$ dimers are preserved, both with their K^+ cations in equatorial disposition (one of them is 31.3 kcal/mol more stable than the other), (3) the most stable equatorial conformation is 60.3 kcal/mol more stable than the axial conformation, (4) the closed-shell singlet optimum geometry of the π-TCNE$_2^{2-}$ dimers for the K_2TCNE_2 aggregate in their equatorial conformation agrees well with that found in crystals, (5) the dominant energetic component in the equatorial conformation is the electrostatic cation–anion interaction, and (6) there is a non-negligible dispersion component in the interaction energy, required to make the closed-shell singlet structure more stable than the open-shell structure, in good agreement with the experimental data.

Acknowledgments

The authors acknowledge the allocation of computer time by CESCA/CEPBA and BSC. IGY also thanks the Spanish Science and Education Ministry for his Ph.D. grant.

References

1. Novoa, J. J.; Lafuente, P.; Del Sesto, R. E.; Miller, J. S. Angew Chem Int Ed 2001, 40, 2540.
2. Del Sesto, R. E.; Sommer, R. D.; Miller, J. S. Cryst Eng Comm 2002, 4, 47.
3. Del Sesto, R. E.; Botoshansky, M.; Kaftory, M.; Miller, J. S. Cryst Eng Comm 2002, 4, 106.
4. Novoa, J. J.; Lafuente, P.; Del Sesto, R. E.; Miller, J. S. Cryst Eng Comm 2002, 4, 373.

5. Del Sesto, R. E.; Miller, J. S.; Lafuente, P.; Novoa, J. J. Chem—Eur J 2002, 8, 4894.
6. Ganesan, V.; Rosokha, S. V.; Kochi, J. K. J Am Chem Soc 2003, 125, 2559.
7. Lu, J. M.; Rosokha, S. V.; Kochi, J. K. J Am Chem Soc 2003, 125, 12161.
8. Jakowski, J.; Simons, J. J Am Chem Soc 2003, 125, 13334.
9. Jung, Y. S.; Head-Gordon, M. Phys Chem Chem Phys 2004, 6, 2008.
10. Block, H.; Ruppert, K.; Fenske, D.; Goesmann, H. Z. Anorg Allg Chem 1991, 595, 275.
11. Szabo, A.; Ostlund, N. S. Modern Quantum Chemistry; McMillan: London, 1982.
12. (a) Becke, A. D. J Chem Phys 1993, 98, 5648; (b) Lee, C.; Yang, W.; Parr, R. G. Phys Rev B 1988, 37, 785.
13. Carvajal, M. A.; García-Yoldi, I.; Novoa, J. J. J Mol Struct (Theochem) 2005, 727, 181.
14. Nakano, H.; Nakayama, K.; Hirao, K.; Dupuis, M. J Chem Phys 1997, 106, 4912.
15. Roos, B. O.; Andersson, K.; Fulscher, M. K.; Malmqvist, P.-A.; Serrano-Andres, L.; Pierloot, K.; Merchan, M. Adv Chem Phys 1996, 93, 219.
16. Allen, F. H. Acta Crystallogr Sect B 2002, 58, 380.
17. Parr, R. G.; Yang, W. Density-Functional Theory of Atoms and Molecules; Oxford University Press: Oxford, 1989.
18. Noodleman, L. J Chem Phys 1981, 74, 5737.
19. Noodleman, L.; Davidson E. Chem Phys 1986, 109, 131.
20. Goldstein, E.; Beno, B.; Houk, K. N. J Am Chem Soc 1996, 118, 6036.
21. Ditchfield, R.; Hehre, W. J.; Pople, J. A. J Chem Phys 1971, 54, 724.
22. Frisch, M. J.; Trucks, G. W.; Schlegel, H. B.; Scuseria, G. E.; Robb, M. A.; Cheeseman, J. R.; Montgomery, Jr., J. A.; Vreven, T.; Kudin, K. N.; Burant, J. C.; Millam, J. M.; Iyengar, S. S.; Tomasi, J.; Barone, V.; Mennucci, B.; Cossi, M.; Scalmani, G.; Rega, N.; Petersson, G. A.; Nakatsuji, H.; Hada, M.; Ehara, M.; Toyota, K.; Fukuda, R.; Hasegawa, J.; Ishida, M.; Nakajima, T.; Honda, Y.; Kitao, O.; Nakai, H.; Klene, M.; Li, X.; Knox, J. E.; Hratchian, H. P.; Cross, J. B.; Bakken, V.; Adamo, C.; Jaramillo, J.; Gomperts, R.; Stratmann, R. E.; Yazyev, O.; Austin, A. J.; Cammi, R.; Pomelli, C.; Ochterski, J. W.; Ayala, P. Y.; Morokuma, K.; Voth, G. A.; Salvador, P.; Dannenberg, J. J.; Zakrzewski, V. G.; Dapprich, S.; Daniels, A. D.; Strain, M. C.; Farkas, O.; Malick, D. K.; Rabuck, A. D.; Raghavachari, K.; Foresman, J. B.; Ortiz, J. V.; Cui, Q.; Baboul, A. G.; Clifford, S.; Cioslowski, J.; Stefanov, B. B.; Liu, G.; Liashenko, A.; Piskorz, P.; Komaromi, I.; Martin, R. L.; Fox, D. J.; Keith, T.; Al-Laham, M. A.; Peng, C. Y.; Nanayakkara, A.; Challacombe, M.; Gill, P. M. W.; Johnson, B.; Chen, W.; Wong, M. W.; Gonzalez, C.; and Pople, J. A. Gaussian-03, Revision-C. 02; Gaussian, Inc: Wallingford, CT, 2004.
23. Schmidt, M. W.; Baldridge, K. K.; Boatz, J. A.; Elbert, S. T.; Gordon, M. S.; Jensen, J. H.; Koseki, S.; Matsunaga, N.; Nguyen, K. A.; Su, S. J.; Windus, T. L.; Dupuis, M.; Montgomery, J. A. J Comput Chem 1993, 14, 1347.
24. Boys, S. F.; Bernardi, F. Mol Phys 1970, 19, 553.
25. van Duijneveldt, F. B.; van Duijneveldt-van de Rijdt, J. G. C. M.; van Lenthe, J. H. Chem Rev 1994, 94, 1873.
26. Novoa, J. J.; Planas, M.; Whangbo, M.-H. Chem Phys Lett 1994, 225, 240.